Protein Science (2000), *9*:1503–1518. Cambridge University Press. Printed in the USA.

Chemical cross-linking with thiol-cleavable reagents combined with differential mass spectrometric peptide mapping—A novel approach to assess intermolecular protein contacts

KEIRYN L. BENNETT,[1,4] MARTIN KUSSMANN,[1,3,4] PER BJÖRK,[2] MAGDALENA GODZWON,[2] MARIE MIKKELSEN,[1] POUL SØRENSEN,[2] AND PETER ROEPSTORFF[1]

[1]Department of Molecular Biology, University of Southern Denmark, Campusvej 55, DK-5230 Odense M, Denmark
[2]Active Biotech Research AB, Scheelevägen 22, SE-220 07 Lund, Sweden

(RECEIVED July 19, 1999; FINAL REVISION March 24, 2000; ACCEPTED May 25, 2000)

Abstract

The intermolecular contact regions between monomers of the homodimeric DNA binding protein ParR and the interaction between the glycoproteins CD28 and CD80 were investigated using a strategy that combined chemical cross-linking with differential MALDI-MS analyses. ParR dimers were modified in vitro with the thiol-cleavable cross-linker 3,3′-dithio-*bis*(succinimidylproprionate) (DTSSP), proteolytically digested with trypsin and analyzed by MALDI-MS peptide mapping. Comparison of the peptide maps obtained from digested cross-linked ParR dimers in the presence and absence of a thiol reagent strongly supported a "head-to-tail" arrangement of the monomers in the dimeric complex. Glycoprotein fusion constructs CD28-IgG and CD80-F_{ab} were cross-linked in vitro by DTSSP, characterized by non-reducing SDS-PAGE, digested in situ with trypsin and analyzed by MALDI-MS peptide mapping (± thiol reagent). The data revealed the presence of an intermolecular cross-link between the receptor regions of the glycoprotein constructs, as well as a number of unexpected but nonetheless specific interactions between the fusion domains of CD28-IgG and the receptor domain of CD80-F_{ab}. The strategy of chemical cross-linking combined with differential MALDI-MS peptide mapping (± thiol reagent) enabled localization of the interface region(s) of the complexes studied and clearly demonstrates the utility of such an approach to obtain structural information on interacting noncovalent complexes.

Keywords: cross-linking; DNA-binding protein; glycoprotein; mass spectrometry; noncovalent interactions

The formation of noncovalent complexes by macromolecules is one of the most important molecular processes in biology (Ayed et al., 1998), and all biological systems are regulated by integrated protein–protein and/or protein–DNA interactions. Such regulation is a mandatory requirement of normal cellular activity. The primary objective in understanding the function of integrated systems is to characterize the noncovalent interactions between individual components at the molecular level. Established methods for studying protein complexes are severely limited by the quantity of protein required for the analyses (X-ray crystallography), limited mass range (NMR spectroscopy), poor specificity (ultracentrifugation), and low mass resolution (gel electrophoresis). Moreover, the methods are generally time consuming and tedious. Therefore, there is an increasing need for a rapid, specific, and sensitive method for characterizing protein–protein interactions. The study of intact, noncovalent protein complexes by ESI-MS has received considerable interest in the last decade and numerous literature is available on this topic (Loo, 1997). More recently, "first laser shot" MALDI-MS analyses have shown promise for investigating noncovalent protein structures (Rosinke et al., 1995; Cohen et al., 1997).

In addition to studying native noncovalent complexes, it is possible to chemically intervene via the introduction of a cross-linker

Reprint requests: Keiryn L. Bennett, Protein Research Group, Department of Molecular Biology, University of Southern Denmark, Campusvej 55, DK-5230 Odense M, Denmark; e-mail: bennett@pr-group.sdu.dk.
[3]Current address: Cerbios-Pharma S.A., Via Pian Scairolo 6, CH-6917 Barbengo, Switzerland.
[4]These authors contributed equally to this work.

Abbreviations: HCCA, 4-hydroxy-α-cyano-cinnamic acid; DHB, 2,5-dihydroxybenzoic acid; SA, sinapic acid; CH_3CN, acetonitrile; MALDI-MS, matrix-assisted laser desorption ionization mass spectrometry; Q-TOF, quadrupole time of flight; MS-MS, tandem mass spectrometry; ESI-MS, electrospray ionization mass spectrometry; DTT, 1,4-dithiothreitol; DTSSP, 33-dithio-*bis*[sulfosuccinimidyl-propionate]; IgG, immunoglobulin; F_{ab}, antigen-binding fragment; IgV, immunoglobulin variable-like; IgC_2, immunoglogulin constant-like; PBS, phosphate-buffered saline; SDS-PAGE, sodium dodecylsulfide polyacrylamide gel electrophoresis; TFA, trifluoroacetic acid.

that covalently links subunits in a protein complex or interacting protein species. Such intervention can assist in the study of higher order protein structure and has the distinct advantage that noncovalently associated proteins are stabilized by the inclusion of a cross-linker. Chemical cross-linking of noncovalent protein complexes and analysis of the cross-linked species by SDS-PAGE has long been employed in biochemistry laboratories to determine the stoichiometry of the constituent monomers (Davies & Stark, 1970; Jung & Moroi, 1983). Cross-linking followed by MALDI-MS analysis has more recently been utilized to determine the stoichiometry of noncovalent protein complexes (Farmer & Caprioli, 1998; Helin et al., 1999), and some studies have extended this to proteolytic digestion of the crosslinked species and subsequent identification of the linked peptides (Artemyev et al., 1993; Ngai et al., 1994; Haniu et al., 1995; Rossi et al., 1995; Vater et al., 1996; Yang et al., 1996; Yu et al., 1997; Hegyi et al., 1998; Mills et al., 1998; Scaloni et al., 1998). One group has utilized photoactivatible thiol-cleavable cross-linkers to covalently link a protein and an interacting peptide, followed by MALDI-MS analysis of the proteolytic digest of the cross-linked species (Kaufmann et al., 1995; Machold et al., 1995). To date, however, there is no report in the literature that utilizes a thiol-cleavable cross-linker to covalently link protein subunits or interacting molecules, and differential MALDI-MS peptide mapping (± thiol reagent) to determine the contact sites in the noncovalent complex.

Strategy

The general strategy we have employed for cross-linking interacting protein species followed by mass spectrometric peptide mapping is illustrated in Figure 1. The protein assembly is incubated with the thiol-cleavable cross-linker to form a stable covalently-linked complex. The cross-linked system is proteolytically digested and analyzed by MALDI-TOF-MS. The peptide mixture of the covalently linked protein complex is also treated with a thiol reagent to cleave the cross-linked species and the sample re-analyzed by MALDI-TOF-MS. Peptide maps obtained prior to and following reduction of the thiol linker are compared. Signals that are not observed after reduction of the linker are assigned as putative cross-linked peptides. Confirmation is obtained if one or both halves of the cross-linked peptides are observed in the peptide map following reduction of the thiol linker. This approach is straightforward for simple models, however, more complicated systems require additional methodological steps. Under some circumstances, it may be necessary to reduce complex peptide mapping data derived from interaction studies to a simpler data set prior to interpretation. This is achieved by stepwise subtraction of MALDI-TOF-MS peptide maps. Thus, as shown in Figure 2, the peptides observed in the digest of the unmodified proteins are subtracted from the peptide map of the cross-linked species. The peptides observed from incubation of the individual interacting proteins

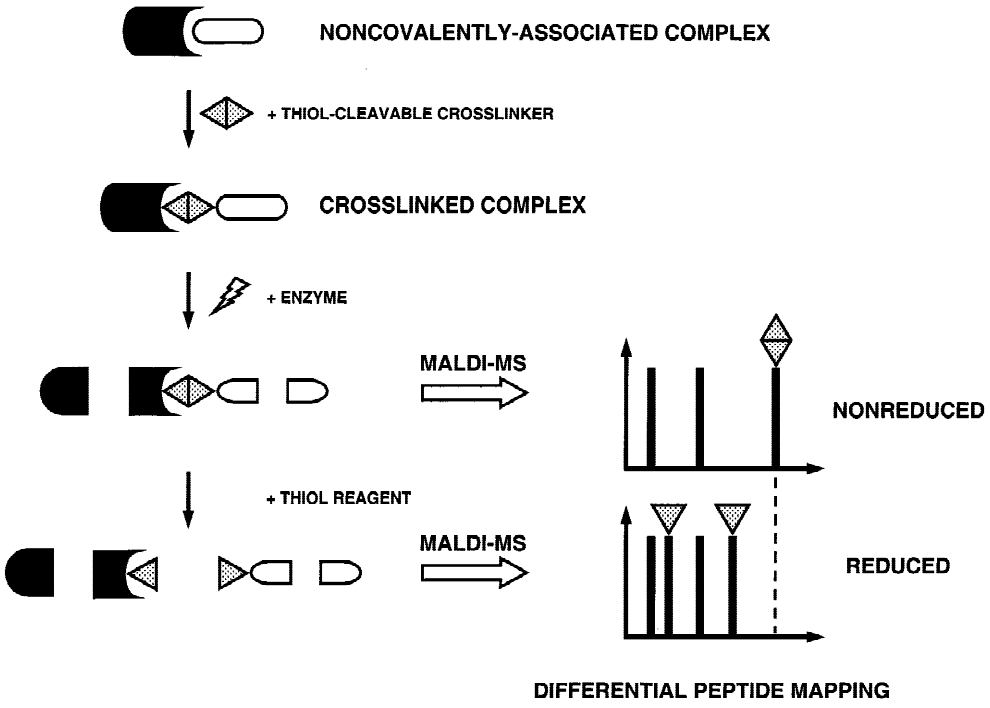

Fig. 1. Analytical strategy for chemical cross-linking with thiol-cleavable reagents (e.g., DTSSP) and differential peptide mapping by MALDI-TOF-MS. Noncovalently associated protein complexes are incubated with the cross-linking reagent to form a stable covalent complex. The complex is proteolytically digested and the peptides analyzed by MALDI-MS. The same peptide digest is incubated with a thiol-reagent (e.g., DTT) and reanalyzed by MALDI-MS. Peptide maps obtained prior to, and following reduction of the thiol-linker are compared. Peptides that are not observed in the spectrum following reduction are assigned as putative cross-links. Confirmation of the cross-link is obtained if the reduced peptide halves are observed after reduction.

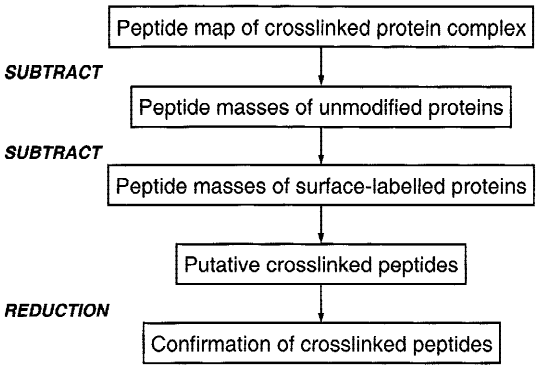

Fig. 2. Flow diagram showing how complicated MALDI-MS peptide maps obtained from cross-linking experiments can be reduced to a simpler data set to facilitate interpretation. The peptide masses from the unmodified proteins are subtracted from the peptide maps of the cross-linked proteins. The peptide masses of the proteins incubated alone with the cross-linker (i.e., surface-labeled proteins) are subtracted from the remaining peptide signals. The final peptides are assessed for putative cross-links. Confirmation is obtained if the peptide signal is not observed after reduction, and peptide signals corresponding to the reduced halves of the assigned cross-link are evident.

with the cross-linker (i.e., surface-labeled but not cross-linked) are also subtracted. The remaining peptides are assigned as putatively cross-linked peptides. Confirmation of the assignment is achieved by treatment of the digest with a thiol reagent. By following this protocol, complex MALDI-TOF-MS peptide maps are easily reduced to a simpler data set that can be readily interpreted and cross-linked peptides identified.

We present here a combined method for investigating the intermolecular contact regions between interacting proteins using the thiol-cleavable cross-linker 3,3′-dithio-*bis*(succinimidylproprionate) (DTSSP) (Lomant & Fairbanks, 1976). DTSSP is a water-soluble, homo-bifunctional, thiol-cleavable *N*-hydroxysuccinimide ester that reacts rapidly and specifically with primary amines (ϵ-amino group of lysine residues and N-terminal α-amino group) to form covalent cross-links with the concomitant release of *N*-hydroxysuccinimide (Fig. 3). The cross-linker has a spacer distance that enables cross-linking of amino groups up to 12 Å apart. The successful incorporation of a DTSSP-generated intermolecular or intramolecular cross-link increases the (average) mass of the protein (or protein complex) by 174.24 Da (Fig. 3, reactions 1 and 3). If a lysine residue is not located in the vicinity of the unconjugated end of a cross-linker, hydrolysis of the second moiety is inherent. Such a modification increases the (average) mass of the protein by 192.26 Da and provides additional structural information on the surface accessibility of the lysine residues (Fig. 3, reaction 4). After reduction of the cross-linker thiol group, the intermolecular link yields two now-separated components each with the reduced form of the linker (average mass increment of 88.130 Da). The intramolecular cross-link yields two reduced linker halves on the same molecule, and the hydrolyzed moiety results in a single reduced linker. In addition to amine acylation, a minor reaction can occur in which free thiol groups in the protein can be reversibly modified by disulfide interchange with the cross-linker (Fig. 3, reaction 2). Modification increases the (average) mass of the protein by 104.13 Da, but following reduction the protein reverts to the unmodified mass (i.e., no mass increment is evident).

Proteins

The strategy outlined above was used to (1) probe the intermolecular contact region between monomers of the homodimeric DNA-binding protein ParR and (2) characterize the interaction between the glycoproteins CD28 and CD80.

The homodimeric DNA-binding protein ParR

The ParR protein is a 13.3 kDa DNA-binding protein that exists exclusively in solution as a dimer (M. Dam & K. Gerdes, unpubl. obs.), and plays an integral role in the in the segregation (or partitioning) of newly replicated bacterial plasmids during cell division (Jensen et al., 1998). No X-ray crystallography or molecular modeling data are available for the ParR dimer. Nonetheless, the propensity of ParR monomers to form dimers is an attractive and simple model system to assess the feasibility of protein cross-linking combined with differential MALDI-MS peptide mapping to investigate the three-dimensional structure of a protein complex. More specifically, it is envisaged that with this approach the region(s) of the ParR monomers that are actively involved in the protein–protein interaction to form the dimeric species will be identified.

Glycoproteins CD28 and CD80

The CD80 (B7-1) ligand is expressed on antigen-presenting cells, whereas the expression of its receptor CD28 is restricted to T-lymphocytes. The interaction between these cell–surface proteins complement signaling through the T-cell receptor and constitute the dominant costimulatory pathway of the immune response. This interaction is essential for achieving full T-cell proliferation and activation (Greenfield et al., 1998). CD28 and CD80 are type I membrane-bound receptors and are members of the immunoglobulin superfamily. The extracellular region of CD80 is a glycoprotein ($M_r \sim 45$ kDa) with eight consensus sites for *N*-linked glycosylation. It contains an Ig variable-like (IgV) and an Ig constant-like (IgC_2) domain. The extracellular domain of CD28 is also a glycoprotein (two chain disulfide-linked homodimer, monomeric $M_r \sim 35$ kDa), with five consensus sites for *N*-linked glycosylation per monomer. Both chains are composed of a single IgV domain that mediates binding to CD80. The three-dimensional structure of the homologous receptor CTLA-4 (CD152), with ~30% sequence identity, was recently solved (Metzler et al., 1997). The noncovalent interaction between recombinant fusion constructs of human CD28 and CD80 was studied using the method and strategy outlined above.

Results and discussion

Homodimeric DNA-binding protein ParR

Analysis of intact ParR dimers by MALDI-MS and SDS-PAGE

ParR dimers were chemically cross-linked in solution with DTSSP at molar ratios of protein to cross-linking agent ranging from an equimolar to a 50-fold molar excess. The cross-linking reactions were monitored by MALDI-TOF-MS and nonreducing 1D-SDS-PAGE prior to and following reduction of the thiol linker (Fig. 4). The presence of the intact ParR dimer ($M_r \sim 27$ kDa) and quantitative reduction to the monomeric form were confirmed by both techniques. A total of 0.75–1 nmol ParR was used to optimize the cross-linking conditions. Illustrated in Figure 4A–C are the MALDI-

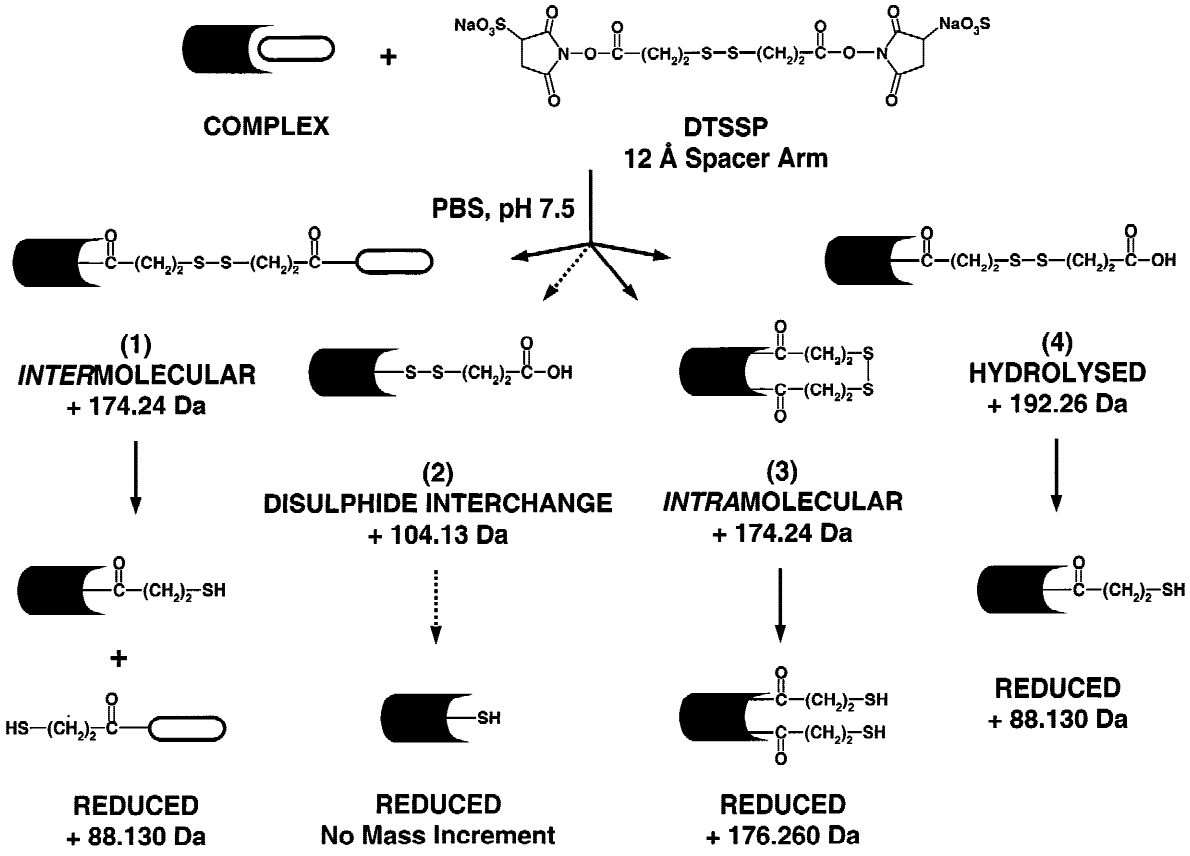

Fig. 3. Modification of a protein complex under physiological conditions with 3,3′-dithio-*bis*[sulfosuccinimidyl-propionate] (DTSSP). Three major reaction pathways are possible: (1) the cross-linker reacts with lysine residues on both of the interacting proteins to form the desired intermolecular cross-link; (2) the cross-linker reacts with two lysine residues within the same molecule to form an intramolecular cross-link; and (3) the complex reacts with the cross-linker, but no lysine residue is available to form the cross-link and the unconjugated end of the cross-linker hydrolyzes. Treatment of all three species with a thiol reagent results in the cleavage of the disulfide bridge. The intermolecularly cross-linked proteins are now separated, and each has a single addition of the reduced form of the cross-linker; the intramolecularly cross-linked species has two additions of the reduced cross-linker and the hydrolyzed moiety is converted to the reduced form. In addition to the major pathways, there is a minor reaction (2) in which the disulfide component of the cross-linker interchanges with cysteine residues in the protein. Following reduction, the modification is removed and no mass increment is observed on the protein.

TOF mass spectra of the native ParR monomer (Fig. 4A), the ParR dimer cross-linked with DTSSP at a molar ratio of protein to cross-linker of 1 to 10 (Fig. 4B) and the cross-linked ParR dimer reduced by DTT (Fig. 4C). Shown inset in Figure 4A is the 1D-SDS-PAGE obtained by cross-linking ParR dimers at molar ratios of 1 to 1, 1 to 10, and 1 to 50, in the absence (lanes 3–5) and presence (lanes 7–9) of a thiol reagent. Lanes 2 and 6 are unmodified ParR ± thiol reagent. Cross-linking of ParR monomers was observed at molar ratios of protein to linker of 1 to 10 or greater. At a molar concentration of ParR to reagent below 1 to 10, dimer formation was incomplete (e.g., lane 3). In Figure 4A, the predominant molecular species is the $[ParR+H]^+$ ion. In addition, there is a small contribution from the $[ParR+ParR+H]^+$ ion. This presumably represents formation of a dimeric species during the MALDI ionization process rather than conservation of the ParR dimer from solution. The important point to note from the spectrum is that the proportion of dimer is markedly reduced compared to the contribution from the singly charged monomer. Following cross-linking of the dimer in solution, the major ion is now the ParR dimer $[ParR+linker+ParR+H]^+$ (Fig. 4B). The doubly charged $[ParR+linker+ParR+2H]^{2+}$ ion is also evident. The molecular ions in the spectrum are particularly broad. The combination of intra- and intermolecular cross-links; surface modification by hydrolyzed cross-linkers; and disulfide interchange of the cross-linker with cysteine residues all contribute to the heterogeneity of the ParR dimer. The resolution of linear mode MALDI-TOF-MS does not allow the various modifications to be observed, and thus an average mass is obtained. Nonetheless, it is apparent from this spectrum that cross-linking of the ParR monomers in solution to form a stable dimeric species was accomplished. MALDI-MS analysis of protein subunits linked by a reagent containing a disulfide bridge must be performed using DHB as a matrix. Matrix-induced fragmentation is reduced and the disulfide link is not cleaved during the MALDI process. Analysis of the same sample with sinapic acid resulted in fragmentation of the cross-linked dimer, and only the monomer was observed. The predominant molecular species following reduction of intra- and intermolecular cross-links and hydrolyzed cross-linker by DTT (Fig. 4C) is the $[ParR+H]^+$ ion, as was observed in Figure 4A. Again, there is a small contribution from the $[ParR+ParR+H]^+$ ion. The implication from this is that

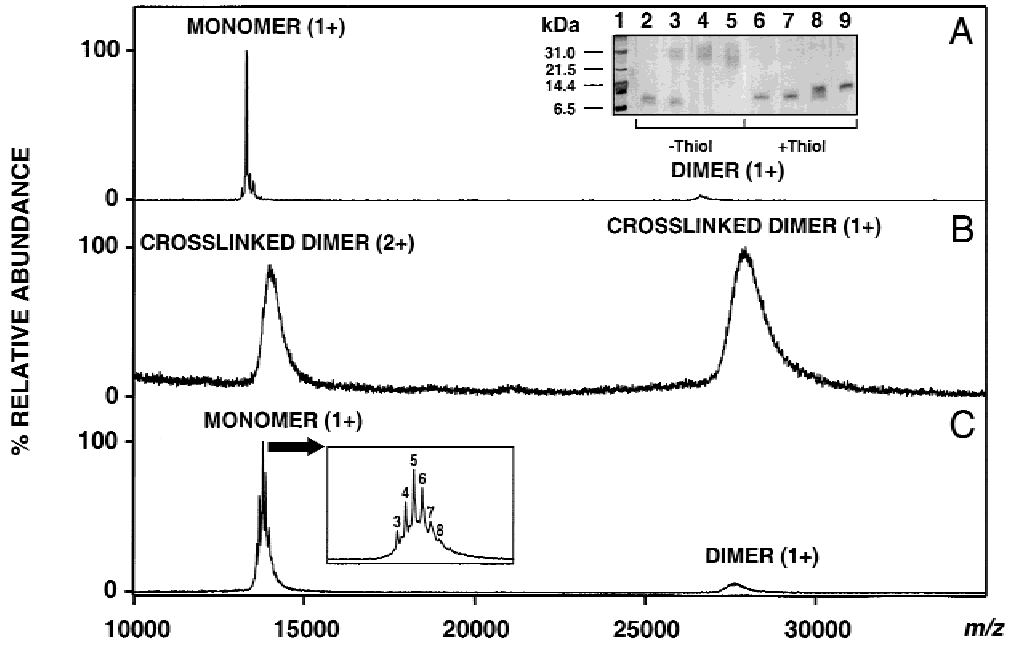

Fig. 4. MALDI-TOF mass spectra of (**A**) unmodified ParR, (**B**) ParR dimers cross-linked in solution with DTSSP at a molar ratio of protein to cross-linker of 1 to 10, and (**C**) cross-linked ParR dimers reduced with DTT. Shown inset in **C** is a magnification of the singly charged ion after reduction with DTT. The number of modifications on the ParR monomer range from three to eight additions of the reduced form of the DTSSP cross-linker, as evidenced by the average mass increments of ~88 Da. Shown inset in **A** is the nonreducing 1D-SDS-polyacrylamide gel electrophoretic characterization of the ParR dimers cross-linked with DTSSP. Lane 1, low-molecular-mass protein markers (carbonic anhydrase, trypsin inhibitor, hen egg-white lysozyme and aprotinin); Lane 2, unmodified ParR; Lane 3, ParR:DTSSP (1:1); Lane 4, ParR:DTSSP (1:10); Lane 5, ParR:DTSSP (1:50); Lane 6, reduced unmodified ParR; Lane 7, reduced ParR:DTSSP (1:1); Lane 8, reduced ParR:DTSSP (1:10); Lane 9, reduced ParR:DTSSP (1:50). The proteins were visualized by silver staining. Matrix for **A** and **C**: SA. Matrix for **B**: DHB. (Note: MALDI-MS analysis of protein subunits linked by a reagent containing a disulfide bridge must be performed using DHB as a matrix. Matrix-induced fragmentation is reduced and the disulfide link is not cleaved during the MALDI process). Accelerating voltage: 25 keV.

a stable covalently linked ParR dimer is no longer present, but has been exclusively converted to the monomer (also evident in Fig. 4A inset, lanes 7–9). The major difference between Figures 4A and 4C is that the ParR monomer is now modified. The heterogeneous ParR dimer is converted into a surface-labeled homogeneous monomer with three to eight modifications (discussed in detail below) as observed by mass increments of ~88 Da (shown inset). The data from the cross-linking of the intact ParR monomers are summarized in Table 1.

Tryptic digestion of cross-linked ParR dimers and differential MALDI-MS peptide mapping

ParR dimers cross-linked with a 50-fold excess of DTSSP were digested in solution by trypsin, and the resultant peptides analyzed by MALDI-TOF-MS prior to and following reduction by DTT (Figs. 5A and 5B, respectively). The data obtained from differential peptide mapping revealed the presence of a single intermolecular cross-link and two intramolecular cross-links. Intermolecular cross-links are defined as links formed between peptides in different monomers. Intramolecular cross-links are defined as cross-links formed within the same monomer, or more specifically, the same peptide. An important issue to bear in mind when cross-linking homodimeric complexes is that it can be difficult to unequivocally ascertain if an observed cross-link has formed between two different regions of the same protein molecule, or between two different regions of two *different* molecules. Nonetheless, if the presence of the intact cross-linked dimer has been confirmed by SDS-PAGE and/or MALDI-MS and sequence coverage is high (as is the case in this investigation, see below), then ions correspond-

Table 1. *Expected and observed average $[M+H]^+$ value for the ParR monomer and the observed $[M+H]^+$ value for the DTSSP-cross-linked ParR dimer*[a]

	Observed mass $[M+H]^+$	Expected mass $[M+H]^+$
ParR monomer	13,326	13,326
Crosslinked ParR dimer	27,896	—
ParR monomer + 1 reduced DTSSP	Not observed	13,414
+ 2 reduced DTSSP	Not observed	13,503
+ 3 reduced DTSSP	13,589	13,591
+ 4 reduced DTSSP	13,676	13,679
+ 5 reduced DTSSP	13,764	13,767
+ 6 reduced DTSSP	13,853	13,855
+ 7 reduced DTSSP	13,944	13,943
+ 8 reduced DTSSP	14,034	14,031

[a]An expected mass for the dimer could not be assigned due to the combination of multiple cross-links and surface labels. Also included are the average expected and observed $[M+H]^+$ values resulting from reduction of the cross-linked dimer.

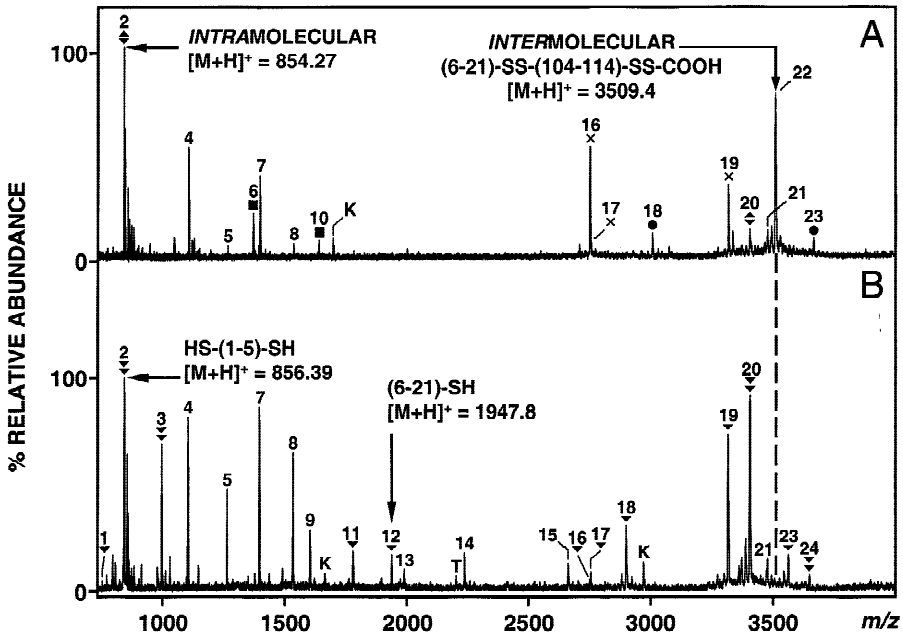

Fig. 5. MALDI-TOF-MS peptide map of ParR dimers cross-linked in solution by DTSSP at a molar ratio of protein to DTSSP of 1 to 50. Samples were digested overnight at 37 °C with 4% (w/w) trypsin. Peptide map (**A**) prior to, and (**B**) following DTT reduction of the thiol linker. Note in particular the disappearance of the peak at *m/z* 3,509.4 (**A**) (corresponds to an intermolecular cross-link between peptide 6–21 and peptide 104–114 plus the addition of a hydrolyzed DTSSP moiety), and the appearance of the peak at *m/z* 1,947.8 (**B**) (peptide 6–21 plus the addition of a reduced DTSSP moiety). This suggests that peptides 6–21 and 104–114 were joined by the cross-linker prior to DTT reduction. The ion corresponding to peptide 104–114 plus two additions of the reduced form of the cross-linker (m/z_{exp} 1,456.6) was not detected in the MALDI mass spectrum. Note also the peptide at *m/z* 854.27 (**A**), which corresponds to an intramolecular cross-link formed between the ϵ-amino group of K^4 and the N-terminal amino group of M^1. Confirmation of this assignment was achieved by the disappearance of the signal at *m/z* 854.27, and the appearance of a new peptide at *m/z* 856.39 (**B**). Unmodified peptides are not labeled; (⬍⬍) peptide plus an intrapeptide cross-link; (●) peptide plus a hydrolyzed DTSSP moiety; (▼) peptide plus a reduced DTSSP moiety; (■) peptide plus a disulfide-interchanged DTSSP moiety; (×) peptide plus a fragmented DTSSP moiety and a fragmented disulfide-interchanged DTSSP moiety. Molecular ions from trypsin autoproteolysis products and human cytoskeletal keratin are labeled T and K, respectively. Ion numbers are correlated with the data shown in Tables 2 and 3. Matrix: HCCA. Accelerating voltage: 20 keV.

ing to intermolecularly cross-linked peptides can be assigned with a high degree of certainty.

The molecular ion at *m/z* 3,509.4 (m/z_{exp} 3,508.0) (22, Fig. 5A) corresponds in mass to an intact intermolecular cross-link between peptide 6–21 from one monomer to peptide 104–114 from the second monomer, plus the addition of a hydrolyzed DTSSP moiety. Peptide 6–21 has one lysine residue (K^{11}), whereas peptide 104–114 has two lysine residues available for modification ($K^{109}$and K^{110}). It is presumed that the ϵ-amino group of the C-terminal lysine residues (i.e., K^{21} and K^{114}) are not altered by DTSSP, as it is improbable that trypsin would cleave after the modified residue. Following reduction, the peak at *m/z* 3,509.4 was no longer evident in the mass spectrum; however, a new peptide at *m/z* 1,947.8 (m/z_{exp} 1,948.0) (12, Fig. 5B) representing peptide 6–21 with a reduced cross-linker modification was apparent. The peptide corresponding to residues 104–114 with two additions of the reduced cross-linker (predicted *m/z* 1,456.6) was not observed in the MALDI mass spectrum. To confirm the presence of the peptide, the unseparated digest was analyzed by quadrupole time-of-flight (Q-TOF) ESI-MS-MS. The doubly charged ion at *m/z* 728.50 (m/z_{exp} 728.80) was isolated by the quadrupole mass filter, collisionally activated with argon and the fragment ions detected by the TOF analyzer. The spectrum in Figure 6 shows the *y*-ion series (Roepstorff & Fohlman, 1984), which confirmed the addition of the reduced form of DTSSP to K^{109} and K^{110} in the sequence S^{104}DEET KKNAMK^{114}. The presence of the second half of the reduced intermolecular cross-link in the tryptic digest was therefore unequivocally determined.

In addition to the intermolecular cross-link, there is evidence of an intramolecular cross-link between the ϵ-amino group of K^4 and the α-amino group of M^1. The peptide at *m/z* 854.27 (m/z_{exp} 854.30) (2, marked by ⬍⬍) corresponds in mass to peptide 1–5 (contains only one lysine residue) plus the addition of an intact cross-link. Reduction of the peptide (2, Fig. 5B) resulted in a peak at *m/z* 856.39 (m/z_{exp} 856.32), 2.1200 Da greater in mass than prior to DTT reduction, thereby confirming the intrapeptide link. The cross-link was validated by the peptide at *m/z* 1,012.4 (m/z_{exp} 1,012.4) (3, Fig. 5B), which corresponds in mass to peptide 1–6 plus the addition of two reduced forms of the cross-linker (M^1 and K^4). The intact cross-link was not observed in Figure 5A at m/z_{exp} 1,010.4, but was apparent in the nonreduced sample analyzed with the matrix DHB (Table 2). A second intrapeptide cross-link is evident in Figure 5A at *m/z* 3,406.6 (m/z_{exp} 3,406.9) (20, marked by ⬍⬍), which corresponds in mass to peptide 7–35 (K^{11} and K^{21}). Following reduction of the cross-linker, the peptide mass increased to *m/z* 3,408.4 (m/z_{exp} 3,408.9), again confirming the presence of an intrapeptide cross-link. Two ions were evident in Figure 5A (18 and 23, marked by ●) that correspond in mass to peptides 79–103

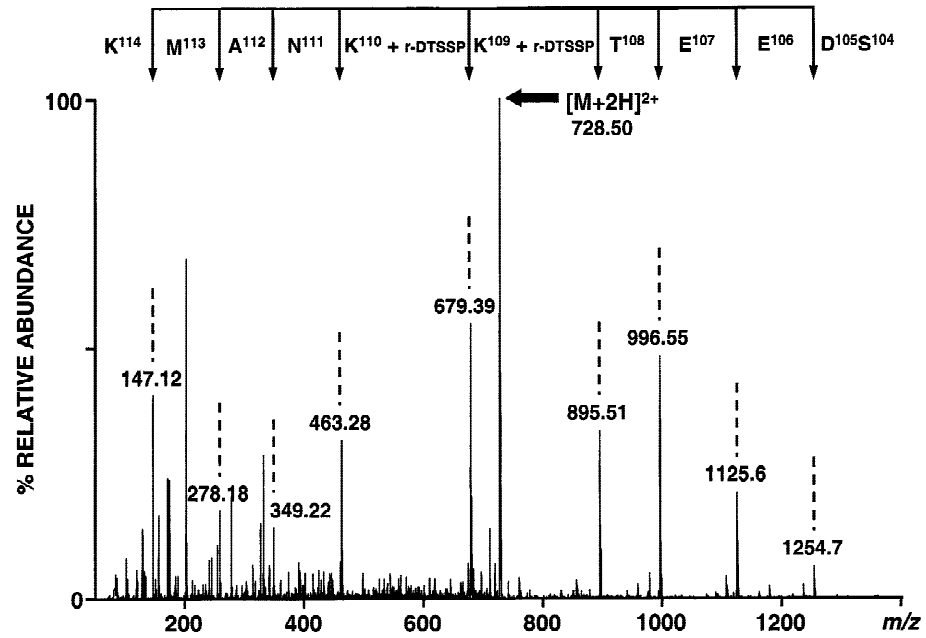

Fig. 6. ESI-MS-MS spectrum of the doubly-charged ion at *m/z* 728.50. The *y*-ion series corresponds to residues 104–114 (SDEET KKNAMK) plus two additions of the reduced form of the DTSSP cross-linker (K^{109} and K^{110}). The presence of the peptide unequivocally confirmed the intermolecular cross-link observed between peptides 6–21 and 104–114. Collision energy: 30 V.

and 7–37 plus one addition of the hydrolyzed form of DTSSP (monoisotopic mass increment 191.99 Da). Confirmation of the assignments was achieved following reduction. Both peptides with the hydrolyzed moiety disappeared and reappeared in Figure 5B with the reduced form of DTSSP (18 and 23, marked by ▼).

Peptides containing a cysteine residue can be modified as a result of disulfide interchange with the cross-linker (monoisotopic mass increment of 103.99 Da). As shown in Figure 5A, the peptides at *m/z* 1,381.7 and 1,649.7 (6 and 10, marked by ■) correspond to peptides 56–66 and 22–35, respectively, plus one addition of the interchanged DTSSP. Both adducts disappeared following reduction with a concomitant increase in relative abundance of the unadducted peptides (5 and 8, Fig. 5B).

It became apparent from the data in Figure 5A that the disulfide bond located in the spacer region of the cross-linker in the nonreduced sample is occasionally cleaved during the MALDI process. The phenomenon of the disulfide bridge cleavage has been previously observed and was attributed to prompt fragmentation or "in-source decay" (Patterson & Katta, 1994). These investigators determined that the flight time of the "pseudomolecular" ions was consistent with cleavage between the sulfur atoms of the cystinyl residue; however, the mass accuracy was not sufficient to unequivocally determine whether the species produced by the fragmentation were protonated at the sulfydryl (–SH). As a consequence of improved mass accuracy, the present study revealed that the ions produced by prompt fragmentation were not protonated at the sulfydryl, but yielded a radical ion (–S·). Thus, modification of a lysine residue by DTSSP followed by prompt fragmentation of the disulfide bridge generated an intact peptide plus the addition of a reduced form of the cross-linker less a hydrogen atom (Fig. 7A). Disulfide interchange of the cross-linker with the cysteine residues followed by prompt fragmentation produced an intact peptide less one hydrogen atom (Fig. 7B). Upon reduction both the sulfur atom of the cysteine residue and the cross-linker are protonated. The mass of the cysteine-containing peptide is thereby restored; and the mass of the lysine-containing peptide plus a fragmented DTSSP moiety is reverted to the mass of the peptide plus a reduced form of the cross-linker.

Ions 16, 17, and 19 (marked with ×) were attributed to peptides 56–78, 12–35, and 7–35, respectively. The observed masses for all three peptides were ~2 Da less than the expected masses considering modification with a reduced form of the cross-linker. The assumption is that the peptides were modified at a lysine residue by DTSSP and at the cysteine residue by disulfide interchange with DTSSP and both disulfide links were fragmented in the MALDI-MS source. Reduction of ion 16, 17, and 19 (Fig. 5B, marked by ▼) protonated both the fragmented sulfydryl residues to give peptides containing one equivalent of the reduced form of the DTSSP cross-linker.

Comparison of the intact ParR dimers vs. the tryptic digest

In the intact cross-linked and reduced ParR, 3–8 additions of the reduced DTSSP moiety were evident (Fig. 4C). The ParR monomer has 10 potential sites for modification by DTSSP, i.e., nine lysine residues and the α-amino group of the N-terminus. Nine residues were partially modified as evidenced from the data from the reduced tryptic digest of the cross-linked dimers (Fig. 5B; Table 3). Only K^{103} was not found modified by DTSSP. Therefore, it is apparent that the eight modifications observed on the intact reduced cross-linked ParR monomer (Fig. 4C) are distributed between nine residues. This is not beyond reason, as many investigators have reported that the incorporation of a modifying group into a protein can result in a population of different molecular species with an equal number of modifying groups but located at different positions (Zappacosta et al., 1997).

Table 2. *Expected and observed [M+H]$^+$ values for the peptides generated from the tryptic digest of the DTSSP-cross-linked ParR dimer, in the absence of a reducing agent*[a]

#	Observed mass $[M+H]^+$	Expected mass $[M+H]^+$	Residue assignment	Sequence assignment	Modification	Modified residues	Matrix
2	854.27	854.30	1–5	MMDKR	Intra-peptide cross-link	M_1-SS-K_4	HCCA
	1,010.1	*1,010.4*	*1–6*	*MMDKRR*	*Intra-peptide cross-link*	*M_1-SS-K_4*	*DHB*
4	1,119.6	1,119.7	41–51	AALTAGLALYR			HCCA
5	1,277.6	1,277.7	56–66	TPFLLCELLTK			HCCA
6	1,381.7	1,381.7	56–66	TPFLLCELLTK	+ ×-DTSSP	C^{61}	HCCA
7	1,407.7	1,407.7	67–78	ETTFSDIVNILR			HCCA
8	1,545.7	1,545.8	22–35	IVCDTLDSIPQGER			HCCA
	1,616.6	*1,615.8*	*41–55*	*AALTAGLALYRQDPR*			*DHB*
10	1,649.7	1,649.8	22–35	IVCDTLDSIPQGER	+ ×-DTSSP	C^{61}	HCCA
	1,794.5	*1,794.8*	*104–117*	*SDEETKKNAMKLIN*	*Intrapeptide cross-link*	*$K^{109/110}$ or $K^{109/114}$ or $K^{110/114}$*	*DHB*
	1,813.0	*1,812.8*	*104–117*	*SDEETKKNAMKLIN*	*+ h-DTSSP*	*K^{109} or K^{110} or K^{114}*	*DHB*
	1,895.1	*1,895.9*	*7–21*	*TIAFKLNPDVNQTDK*	*+ h-DTSSP*	*K^{11}*	*DHB*
	1,985.8	*1,986.8*	*104–117*	*SDEETKKNAMKLIN*	*Intrapeptide cross-link + h-DTSSP*	*K^{109} & K^{110} & K^{114}*	*DHB*
	1,998.7	*1,999.1*	*38–55*	*LNRAALTAGLALYRQDPR*			*DHB*
	2,243.5	*2,244.0*	84–103	*EMADFNSSIVTQSSSQQEQK*			*DHB*
16	2,752.3	2,752.4	56–78	TPFLLCELLTKETTFSDIVNILR	+ f-×-DTSSP + f-DTSSP	C^{61} & K^{66}	HCCA
17	2,756.3	2,756.3	12–35	LNPDVNQTDKIVCDTLDSIPQGER	+ f-×-DTSSP + f-DTSSP	C^{24} & K^{21}	HCCA
18	3,008.2	3,008.3	79–103	SLFPKEMADFNSSIVTQSSSQQEQK	+ h-DTSSP	K^{83}	HCCA
19	3,318.4 (av)	3,318.8 (av)	7–35	TIAFKLNPDVNQTDKIVCDTLDSIPQGER	+ f-×-DTSSP + f-DTSSP	C^{24} & K^{11} or K^{21}	HCCA
20	3,406.6 (av)	3,406.9 (av)	7–35	TIAFKLNPDVNQTDKIVCDTLDSIPQGER	Intrapeptide cross-link	K^{11}-SS-K^{21}	HCCA
21	3,476.8 (av)	3,475.9 (av)	7–37	TIAFKLNPDVNQTDKIVCDTLDSIPQGERSR			HCCA
22	3,509.4 (av)	**3,508.0 (av)**	**6–21 + 104–114**	**RTIAFKLNPDVNQTDK + SDEETKKNAMK**	**Intermolecular cross-link + hDTSSP**	**K^{11}-SS-K^{109} or K^{110}**	**HCCA**
23	3,666.4 (av)	3,668.2 (av)	7–37	TIAFKLNPDVNQTDKIVCDTLDSIPQGERSR	+ h-DTSSP	K^{11} or K^{21}	HCCA

[a] Peptide assignment and sequence are shown as are the modifications on the peptide and the modified residue(s). All $[M+H]^+$ values are monoisotopic unless otherwise stated. The data in boldface were the only *inter*molecular cross-link observed between the ParR monomers. The data shown in normal face are the ions observed using HCCA. The data shown in italics are the *additional* ions that were observed using DHB. (-SS-) denotes the inclusion of a DTSSP cross-link; (h-DTSSP) peptide plus a hydrolyzed DTSSP moiety; (f-DTSSP) peptide plus a fragmented DTSSP moiety; (×-DTSSP) peptide plus a disulfide-interchanged DTSSP moiety; (f-×-DTSSP) peptide plus a fragmented disulfide-interchanged DTSSP moiety; (av) average $[M+H]^+$.

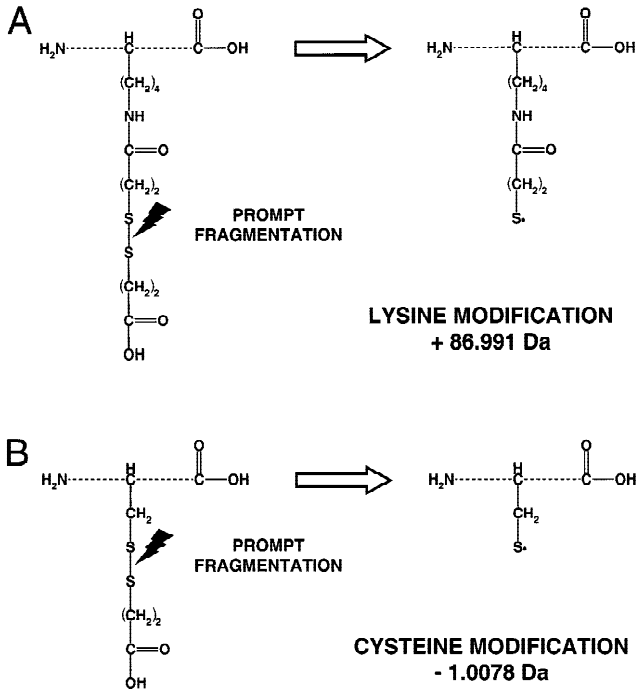

Fig. 7. Prompt fragmentation of DTSSP-modified peptides by MALDI-MS; (**A**) modification of the ϵ-amino group of a lysine residue by DTSSP, followed by cleavage of the disulfide bond–monoisotopic mass *increment* of 86.991 Da (c.f. 87.998 Da for the reduced form of DTSSP); (**B**) modification of a cysteine residue by disulfide interchange with DTSSP followed by cleavage of the disulfide bond–monoisotopic mass *decrement* of 1.0078 Da.

In addition to the peptide maps shown in Figure 5, the digests were also analyzed with DHB (spectra not shown). The results from the tryptic digests prior to and following DTT reduction of the thiol cross-linker with the two matrices are summarized in Tables 2 and 3. Note that the data shown in normal face are the ions observed using HCCA, and the data shown in italics are the additional ions that were observed using DHB. The overall sequence coverage obtained from the peptide maps was 98%. The data demonstrate that by combining chemical protein cross-linking with differential MALDI-TOF-MS peptide mapping, the site of interaction between monomers of the DNA binding protein ParR can be postulated. The formation of a single intermolecular cross-link between a lysine residue in the N-terminal region of one monomer (i.e., K^{11}) and a lysine residue in the C-terminal region of the second monomer (i.e., K^{109} or K^{110}) strongly supports a "head-to-tail" arrangement between the interacting subunits of the ParR dimer.

Receptor-fusion glycoproteins CD28-IgG and CD80-F_{ab}

Analysis of intact CD28-CD80 heterodimers by SDS-PAGE

Picomole quantities of the receptor-fusion glycoproteins CD28-IgG (M_r glycosylated protein ~ 110 kDa) and CD80-F_{ab} (M_r glycosylated protein ~ 90 kDa) were cross-linked in solution by DTSSP, and the reactions monitored by nonreducing 1D-SDS-PAGE. Under optimized conditions, i.e., at a molar ratio of CD28:CD80:DTSSP of 1:2:10,000, DTSSP cross-linking of CD28-IgG and CD80-F_{ab} yielded a well-defined band at ~200 kDa (Fig. 8, lane 4). Protein oligomerization or degradation were not observed. The 200 kDa band represents a dimer yield of ~30%. The semi-quantification of modified vs. unmodified protein by staining of protein bands in gels is often difficult, as cross-linked proteins show a weaker adsorption of the dye than the noncross-linked species (Leffak, 1983). The heterodimer band was not observed under reducing PAGE conditions, which confirmed that CD28-IgG and CD80-F_{ab} were covalently linked by DTSSP (data not shown). Western blot analysis revealed that the DTSSP-generated band was recognized by antibodies against the fusion and receptor regions of CD28-IgG and CD80-F_{ab}, respectively, thereby verifying a functional CD28-CD80 complex (data not shown). Incubation of either CD28-IgG or CD80-F_{ab} with DTSSP did not yield cross-linked homodimeric protein complexes, but rather DTSSP-modified (i.e., surface-labeled) derivatives of the receptor-fusion proteins. Approximately 0.5–1 nmol of each protein was used to obtain the necessary conditions for optimal cross-linking of CD28 and CD80.

In situ tryptic digestion of cross-linked CD28-IgG and CD80-F_{ab} heterodimers and differential MALDI-MS peptide mapping

The 200 kDa silver-stained CD28–CD80 heterodimeric band (~100 ng protein) was excised and digested in situ with trypsin (Shevchenko et al., 1996). Aliquots from the extracted peptide mixture were purified and concentrated according to an in-house nanoscale purification procedure (Gobom et al., 1998) (see Materials and methods). The same sample preparation was used for the protein bands from the unmodified CD28-IgG and CD80-F_{ab}, and the immunoreceptors individually incubated with DTSSP (no cross-linked homodimers observed). The peptide masses derived from the tryptic digests of the unmodified and the DTSSP-labeled glycoprotein constructs (no cross-linking) were subtracted from the peptide map of the digested CD28–CD80 heterodimer (as per Fig. 2). The remaining molecular ions in the spectrum of the complex were assigned as DTSSP-cross-linked peptides. Confirmation of specific CD28–CD80 cross-links was achieved by the disappearance of a peptide signal following reduction. In some instances, as-

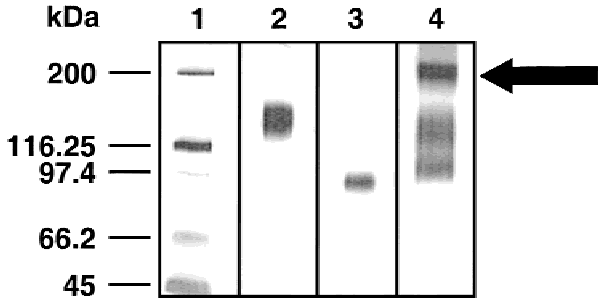

Fig. 8. Nonreducing 1D-SDS-polyacrylamide gel electrophoretic characterization of the recombinant receptor-fusion proteins CD28-IgG and CD80-F_{ab} cross-linked with DTSSP. Lane 1, high-molecular-mass protein markers (myosin, β-galactosidase, phosphorylase b, bovine serum albumin and ovalbumin); Lane 2, unmodified CD28-IgG; Lane 3, unmodified CD80-F_{ab}; Lane 4, DTSSP-cross-linked heterodimer. The proteins were visualized by silver staining. The 200 kDa DTSSP-cross-linked CD28-CD80 heterodimer (marked by the arrow) was excised and digested in situ with trypsin. The peptide mixture obtained was analyzed by MALDI-TOF-MS prior to and following reduction of the thiol linker by DTT.

Table 3. *Expected and observed [M+H]$^+$ ions for the peptides generated from the tryptic digest of the DTSSP-cross-linked ParR dimer, in the presence of a reducing agent*[a]

#	Observed mass $[M+H]^+$	Expected mass $[M+H]^+$	Residue assignment	Sequence assignment	Modification	Modified residues	Matrix
1	768.28	768.31	1–5	MMDKR	+ r-DTSSP	M_1 or K_4	HCCA
2	856.39	856.31	1–5	MMDKR	+ 2 r-DTSSP	M^1 and K^4	HCCA
3	1,012.4	1,012.4	1–6	MMDKRR	+ 2 r-DTSSP	M^1 and K^4	HCCA
4	1,119.6	1,119.7	41–51	AALTAGLALYR			HCCA
5	1,277.7	1,277.7	56–66	TPFLLCELLTK			HCCA
7	1,407.7	1,407.7	67–78	ETTFSDIVNILR			HCCA
8	1,545.7	1,545.8	22–35	IVCDTLDSIPQGER			HCCA
9	1,615.8	1,615.9	41–55	AALTAGLALYRQDPR			HCCA
11	1,791.8	1,791.9	7–21	TIAFKLNPDVNQTDK	+ r-DTSSP	K^{11}	HCCA
	1,796.4	*1,796.8*	*104–117*	*SDEETKKNAMKLIN*	*+ 2 r-DTSSP*	*$K^{109/110}$ or $K^{109/114}$ or $K^{110/114}$*	*DHB*
	1,885.0	*1,884.8*	*104–117*	*SDEETKKNAMKLIN*	*+ 3 r-DTSSP*	*K^{109} & K^{110} & K^{114}*	*DHB*
12	1,947.8	1,948.0	6–21	RTIAFKLNPDVNQTDK	+ r-DTSSP	K^{11}	HCCA
13	1,998.8	1,999.1	38–55	LNRAALTAGLALYRQDPR			HCCA
14	2,243.9	2,244.0	84–103	EMADFNSSIVTQSSSQQEQK			HCCA
15	2,666.4	2,666.4	56–78	TPFLLCELLTKETTFSDIVNILR			HCCA
16	2,754.4	2,754.4	56–78	TPFLLCELLTKETTFSDIVNILR	+ r-DTSSP	K^{66}	HCCA
17	2,758.1	2,758.3	12–35	LNPDVNQTDKIVCDTLDSIPQGER	+ r-DTSSP	K^{21}	HCCA
18	2,904.3	2,904.3	79–103	SLFPKEMADFNSSIVTQSSSQQEQK	+ r-DTSSP	K^{83}	HCCA
19	3,320.5 (av)	3,320.8 (av)	7–35	TIAFKLNPDVNQTDKIVCDTLDSIPQGER	+ r-DTSSP	K^{11} or K^{21}	HCCA
20	3,408.4 (av)	3,408.9 (av)	7–35	TIAFKLNPDVNQTDKIVCDTLDSIPQGER	+ 2 r-DTSSP	K^{11} and K^{21}	HCCA
21	3,476.7 (av)	3,475.9 (av)	7–37	TIAFKLNPDVNQTDKIVCDTLDSIPQGERSR			HCCA
23	3,563.6 (av)	3,564.0 (av)	7–37	TIAFKLNPDVNQTDKIVCDTLDSIPQGERSR	+ r-DTSSP	K^{11} or K^{21}	HCCA
24	3,650.7 (av)	3,652.1 (av)	7–37	TIAFKLNPDVNQTDKIVCDTLDSIPQGERSR	+ 2 r-DTSSP	K^{11} and K^{21}	HCCA

[a]Peptide assignment and sequence are shown, as are the modifications on the peptide and the modified residue(s). All $[M+H]^+$ values are monoisotopic unless otherwise stated. The data shown in normal face are the ions observed using HCCA. The data shown in italics are the *additional* ions that were observed using DHB. (r-DTSSP) peptide plus a reduced DTSSP moiety, (av) average $[M+H]^+$.

signed cross-links were further confirmed by the appearance of one, or both, of the peptides expected from reduction of the assigned cross-link.

Shown in Figures 9A and 9B are corresponding sections of the spectra obtained from the tryptic digest of the CD28–CD80 heterodimeric band prior to and following reduction by DTT. The peptide signal at *m/z* 1,508.7 (m/z_{exp} 1,508.8) (Fig. 9A) corresponds in mass to an intermolecular cross-link formed between peptide 250–255 from CD28-IgG (i.e., K^{253}) and peptide 336–340 from CD80-F_{ab} (i.e., K^{339}). Both lysine residues are located in the fusion domain of CD28-IgG and CD80-F_{ab}, respectively. Following DTT reduction, the ion at *m/z* 1,508.7 was no longer observed (Fig. 9B). The peptides produced from reductive cleavage of the cross-linker (m/z_{exp} 765.41 and m/z_{exp} 746.41, respectively) were not detected, as peptides of mass below approximately *m/z* 1,000 are often suppressed by matrix signals. Nonetheless, the disappearance of a putatively assigned cross-link after thiol treatment is highly indicative that the peptides were linked by the DTSSP moiety. Throughout these analyses, the total sequence coverage obtained for CD28 and CD80 was in the range of 75–80%.

Detailed analyses of the MALDI-MS peptide maps obtained following in situ tryptic digestion of cross-linked CD28-IgG and CD80-F_{ab} revealed the presence of numerous intermolecular cross-links. The results from these experiments are summarized in Table 4 and Figure 10. The receptor region of CD28-IgG and CD80-F_{ab} are represented by the white and gray bars, respectively, and the fusion proteins of both constructs by black bars. The position of the lysine residues involved in intermolecular cross-links for both receptor-fusion glycoproteins are as indicated. The residues in parentheses indicate that a cross-link was observed, but the lysine residue involved could not be assigned. The data were dominated by unexpected but nonetheless specific interactions between the fusion domain of CD28-IgG and the receptor domain of CD80-F_{ab}. One explanation for these interactions is that they are a result of a high avidity association, rather than a low-affinity interaction with a rapid kinetic dissociation rate. Surface plasmon resonance experiments performed with a soluble form of CD80 (sCD80) and CD28-IgG have confirmed the validity of the latter point for the receptor–receptor interaction (van der Merwe et al., 1997). Cross-links between the fusion domain of CD28-IgG and the fusion domain of CD80-F_{ab} were also evident, as were cross-links between the receptor and fusion domains of CD28-IgG, respectively, with the C-terminal region of the fusion domain of CD80-F_{ab}. An additional cross-link between the receptor domains of the glycoproteins was also apparent. The detection of numerous intermolecular cross-links clearly demonstrates the utility of the methodological approach to localize specific, albeit unexpected, sites of interaction between the glycoprotein constructs CD28-IgG and CD80-F_{ab}.

Conclusion

The data presented here demonstrate that the combination of chemical cross-linking with differential MALDI-MS peptide mapping can indicate which region(s) of the protein molecules interact and provide evidence concerning the spatial arrangement of the components in the noncovalent complex. The ParR study showed that the combined approach of chemical cross-linking with MALDI-MS enabled postulation of a model concerning the orientation of the

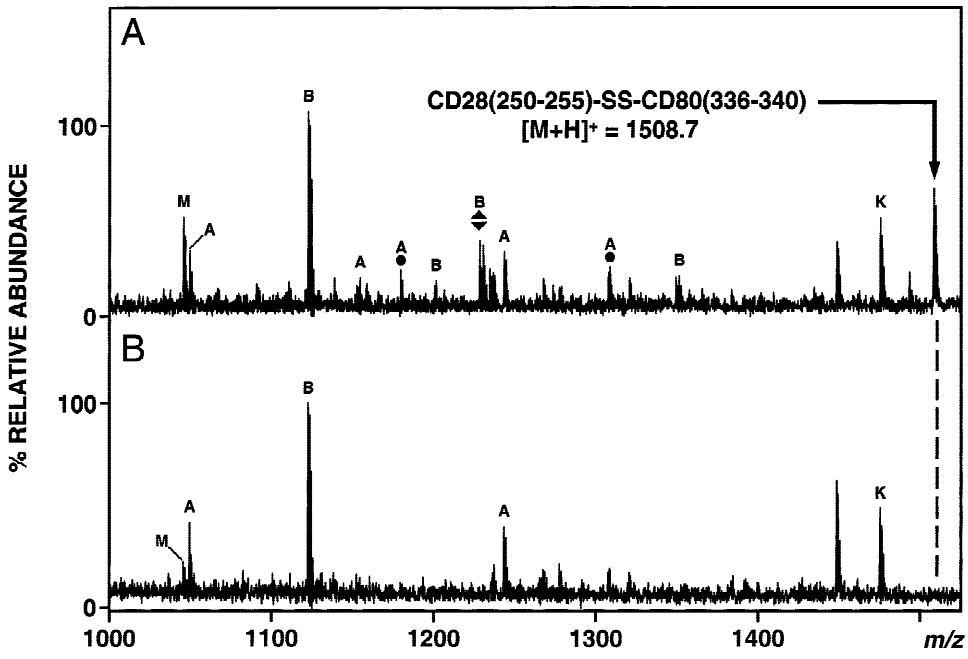

Fig. 9. MALDI-TOF-MS peptide map of CD28-IgG and CD80-F_{ab} cross-linked in solution by DTSSP, characterized by 1D-SDS-PAGE, and digested in situ by trypsin (**A**) prior to and (**B**) following DTT reduction of the thiol linker. The labeled peptide at *m/z* 1,508.7 is attributed to an interaction between the fusion domain of CD28-IgG with the fusion domain of CD80-F_{ab}. The peptides from the putatively assigned cross-link was not observed after treatment with DTT (**B**). Molecular ions from tryptic peptides of unmodified CD28-IgG and CD80-F_{ab} are labeled **A** and **B**, respectively, (●) peptide plus a hydrolyzed DTSSP moiety, (⬍⬍) peptide plus an intrapeptide cross-link. Molecular ions from matrix signals and human cytoskeletal keratin are labeled **M** and **K**, respectively. Matrix: HCCA. Accelerating voltage: 20 keV.

Table 4. *Expected and observed [M+H]$^+$ ions for the DTSSP-cross-linked CD28-IgG and CD80-F$_{ab}$ tryptic peptides*[a]

Observed mass [M+H]$^+$	Expected mass [M+H]$^+$	Residue assignment		Sequence assignment			Cross-linked residues	
		CD28	CD80	CD28	CD80	Modification	CD28	CD80
1,508.7	1,508.8	250–255	336–340	TISKTK	LELKR		253	339
1,815.7	1,815.9	110–120	660–663	SNGTIIHVKGK	VDKK		118	662
2,283.0	2,283.2	250–259	30–36	TISKTKGRPK	IYWQKEK		253 or 255	34
2,383.9	2,383.2	110–120	87–94	SNGTIIHVKGK	YEKDAFKR		118	89 or 93
2,618.3	2,618.3	260–277	35–37	APQVYTIPPPKEQMAKDK	EKK		270 or 275	36
2,631.0 (av)	2,631.2 (av)	260–275	336–340	APQVYTIPPPKEQMAK	LELKR		270	339
2,721.3	2,721.4	164–183	35–37	DVLTITLTPKVTCVVVDISK	EKK		173	36
2,737.6 (av)	2,737.3 (av)	1–6	263–277	NKILVK	NYLTWYQQKPGQPPK		2	271
2,741.1	2,741.3	236–253	90–94	CRVNSAAFPAPIEKTISK	DAFKR		249	93
2,750.7 (av)	2,750.2 (av)	238–253	375–381	VNSAAFPAPIEKTISK	DINVKWK		249	379
2,764.9 (av)	2,765.3 (av)	236–253	336–340	CRVNSAAFPAPIEKTISK	LELKR		249	339
2,927.0 (av)	2,927.6 (av)	260–275	660–667	APQVYTIPPPKEQMAK	VDKKIVPR		270	662 or 663
3,298.3 (av)	3,298.0 (av)	254–270	I–9	TKGRPKAPQVYTIPPPK	VIHVTKEVK	+ hDTSSP	255 or 259	6
3,314.0 (av)	3,314.0 (av)	256–275	375–381	GRPKAPQVYTIPPPKEQMAK	DINVKWK		259 or 270	379
3,340.1 (av)	3,341.0 (av)	271–277	38–56	EQMAKDK	MVLTMMSGDMNIWPEYKNR		275	54
3,387.1 (av)	3,386.7 (av)	250–255	191–211	TISKTK	VNQTFNWNTTKQEHFPDNSAR		253	201
5,330.3 (av)	5,330.4 (av)	217–237	37–56	SVSELPIMHQDWLNGKEFKCR	KMVLTMMSGDMNIWPEYKNR	+ hDTSSP	232 and 235	54
5,346.6 (av)	5,347.1 (av)	256–270	485–513	GRPKAPQVYTIPPPK	QRPGQGLEWIGNIYPSYIYTNYNQEFKDK		259	511

[a]Peptide assignment and sequence are shown as are the modified lysine residues. [M+H]$^+$ values are monoisotopic unless otherwise stated. (h-DTSSP) peptide plus a hydrolyzed DTSSP moiety; (av) average [M+H]$^+$.

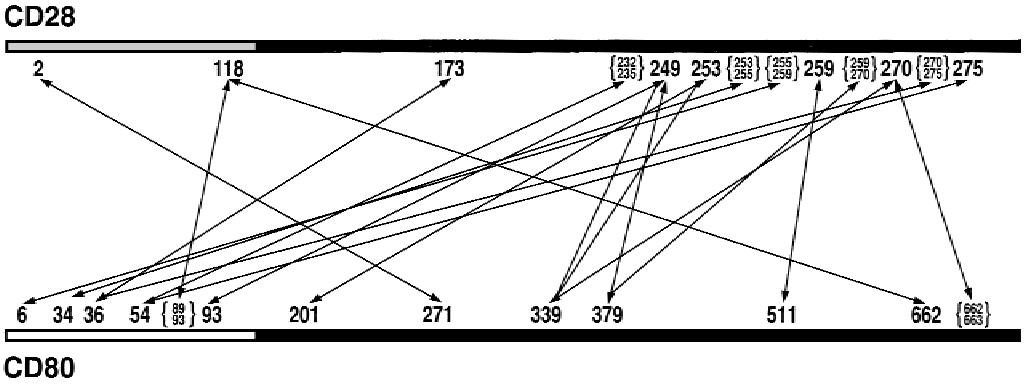

Fig. 10. Summary of the DTSSP cross-links formed between CD28-IgG and CD80-F_{ab} in solution. The numbers represent the position in the protein sequence of the lysine residues involved in the formation of intermolecular cross-links. The residues in parentheses indicate the formation of an intermolecular cross-link but the lysine residue involved could not be assigned. The data revealed significant but largely unexpected interactions between the receptor region of CD80-IgG and the fusion region of CD28-F_{ab}. Gray, CD28 receptor; white, CD80 receptor; black, IgG and F_{ab} fusion proteins, respectively.

monomers of the protein in the dimeric species. Using the same method, the glycoprotein study revealed that specific interactions exist between the CD28-IgG and CD80-F_{ab} constructs. In particular, numerous interactions between the fusion domain of CD28-IgG and the receptor domain of CD80-F_{ab} were evident. The study illustrates possible pitfalls in mimicking protein interactions based exclusively on fusion constructs. To overcome this problem, the binding contribution from the IgG fusion domain may be reduced by immobilizing the glycoprotein constructs (P. Sørensen, A. Rosén, V. Avery, M. Kussmann, K.L. Bennett, M. Norin, P. Roepstorff, & P. Björk, unpubl. obs.). An alternative approach would be to introduce a cleavage site (e.g., thrombin) between the receptor and the fusion domain to reduce interference of the fusion regions with the receptor–receptor interaction.

Current limitations of protein cross-linking and differential peptide mapping are (1) possible steric hindrance of the cross-linking reaction and (2) ion suppression in MALDI-TOF-MS analysis of peptide mixtures. Furthermore, assaying the conservation of the structure of the protein complex after cross-linking remains difficult. To overcome MALDI-MS suppression effects the supplementation of our strategy by simultaneous liquid chromatography separation and mass spectrometry analysis (LC-MS) of proteolytically digested cross-linked proteins is envisaged. Further analysis of putatively cross-linked peptides by tandem mass spectrometry (MS-MS), as initiated in this study, will localize and confirm cross-linked residues. This is particularly important when there are no enzymatic cleavage sites between potentially modified residues. In addition, methods employing affinity-isolation of cross-linked peptides are the subject of continuing studies. This will not only decrease the problems associated with peptide signal suppression in the MALDI-MS spectra, but will also eliminate the need to reduce complex MALDI-TOF-MS peptide maps to a simpler data set.

In conclusion, the data presented here reveal that protein cross-linking and mass spectrometry provides a means to map functionally interacting epitopes of protein complexes. The utility of combining native PAGE with mass spectrometry has been demonstrated as a novel approach for compositional analysis of the spliceosome (Neubauer et al., 1998). By integrating the techniques of PAGE and chemical cross-linking with mass spectrometry, the potential of determining near-neighbor contacts in multicomponent systems is clearly evident and represents the next development in furthering our understanding of protein structure–function relationships.

Materials and methods

Recombinant proteins

ParR dimers were produced and purified by Marie Mikkelsen, Department of Molecular Biology, University of Southern Denmark, Odense M, Denmark.

Receptor-fusion constructs of CD28 and CD80 were provided by Research, Pharmacia & Upjohn AB, Stockholm, Sweden. CD28-IgG and CD80-F_{ab} were expressed in adherent CHO and HEK 293 cells, respectively. CD28-IgG was purified by affinity chromatography on Protein A Sepharose 4 FF (Amersham Pharmacia Biotech, Uppsala, Sweden) followed by gel filtration on Superdex 200 pg (Amersham Pharmacia Biotech). CD80-F_{ab} was purified by gel filtration followed by affinity chromatography on Protein G Sepharose 4 FF (Amersham Pharmacia Biotech).

Chemicals

3,3′-Dithio-*bis*[sulfosuccinimidyl-propionate] (DTSSP) (Pierce, Rockford, Illinois).

The homodimeric DNA-binding protein ParR

Protein cross-linking

ParR dimers were dissolved in 20 mM PBS, pH 7.5 at a concentration of 0.1 mg/mL. DTSSP was dissolved in 20 mM PBS, pH 7.5 at a concentration of 10 mg/mL. The DTSSP was added to the ParR dimers and incubated at ambient temperature for 30 min. Cross-linked samples were not quenched with, for example, Tris or glycine buffers as removal of excess reagent was achieved by desalting the sample after modification.

Tryptic digestion and DTT reduction

Twenty microliters of 2 M urea, 0.1 mM NH_4HCO_3, pH 8.3 were added to the cross-linked ParR dimers. Modified porcine trypsin (Promega Corp., Madison, Wisconsin) was added to 4% (w/w) and the samples digested overnight at 37 °C. Digested samples were divided into two equal portions and one-half of the digest incubated in 50 mM DTT for 30 min at 37 °C to reduce the thiol linker.

SDS-PAGE

Cross-linked ParR dimers were analyzed by nonreducing and reducing 1D-SDS-PAGE (15% polyacrylamide) according to the method of Laemmli (1970). Carbonic anhydrase (M_r 31,000), trypsin inhibitor (M_r 21,500), hen egg-white lysozyme (M_r 14,400), and aprotinin (M_r 6,500) were used as molecular weight markers. Protein bands were visualized by silver staining, and gels were scanned using a ScanJet IIcx (Hewlett-Packard, Palo Alto, California) gel scanner.

Receptor-fusion glycoproteins CD28-IgG and CD80-F_{ab}

Protein cross-linking

To form the noncovalent complex, a 50 μL solution of CD28-IgG (100 nM in 20 mM PBS) and CD80-F_{ab} (200 nM in 20 mM PBS) was preincubated at ambient temperature for 30 min. Five microliters of freshly prepared DTSSP (10 mM in 20 mM PBS) was added to the protein solution and incubated for a further 30 min. The reaction was quenched by the addition of 2.5 μL 1 M Tris-HCl, pH 7.5 and incubation for 15 min.

SDS-PAGE and Western blot analysis

The homogeneity and identity of the CD28-IgG and CD80-F_{ab} recombinant fusion proteins were determined using 1D-SDS-PAGE and Western blotting. The identity of CD28-IgG and CD80-F_{ab} was confirmed by estimating the molecular mass of the Coomassie-stained bands in the gel by comparison with the molecular mass markers. Identified bands were blotted onto nitrocellulose membranes and detected with antibodies specific for CD28 or CD80, and the respective immunoglobulin tags. The homogeneity of the fusion proteins was assessed by scanning the Coomassie-stained gels using an ImageMaster DTS (Pharmacia LKB, Uppsala, Sweden) and was determined as >95% in both cases. Cross-linked proteins were analyzed by nonreducing and reducing 1D-SDS-PAGE (7.5% polyacrylamide) (Laemmli, 1970). Myosin (M_r 200,000), β-galactosidase (M_r 116,250), phosphorylase b (M_r 97,400), bovine serum albumin (M_r 66,200) and ovalbumin (M_r 45,000) were used as molecular mass markers. Protein bands were visualized by silver staining, and gels were scanned using a ScanJet IIcx (Hewlett-Packard, Palo Alto, California) gel scanner. The CD28–CD80 heterodimeric band was characterized by Western blot analysis (according to standard protocols) with antibodies against the fusion and the receptor region of CD28-IgG and CD80-F_{ab}.

In situ tryptic digestion and DTT reduction

The 200 kDa silver-stained band was excised and digested in situ with modified porcine trypsin (Promega Corp., Madison, Wisconsin) according to the method of Shevchenko et al. (1996) with the following modifications. The supernatant from the in situ digest was pooled with the fraction obtained after peptide extraction. Digested samples were lyophilized in a Speed Vac (Savant, Farmingdale, New York), redissolved in ~5 μL 2% formic acid, and divided into two equal portions. Sodium phosphate buffer (7.5 μL 200 mM), pH 8.5 was added to one-half of the digest, and incubated in 100 mM DTT for 30 min at 37 °C to reduce the thiol linker.

Mass spectrometry

MALDI-MS matrices

4-Hydroxy-α-cyano-cinnamic acid (HCCA) (Sigma Pty. Ltd., St. Louis, Missouri), sinapic acid (SA) (Fluka Chemicals, Buchs, Switzerland), 2,5-dihydroxybenzoic acid (DHB) (Hewlett-Packard, Palo Alto, California).

Preparation of MALDI-MS matrices

The tryptic digests of the DTSSP-cross-linked ParR dimers were analyzed with HCCA (10 μg/μL) dissolved in 70% aqueous acetonitrile, 0.1% TFA, and the tryptic digests of DTSSP-cross-linked CD28-IgG and CD80-F_{ab} were analyzed with a saturated solution of HCCA in 45% aqueous acetonitrile, 0.1% TFA, or DHB dissolved in 30% aqueous acetonitrile, 0.1% TFA. Prior to use, 100 μL DHB was lyophilized in a Speed Vac (Savant, Farmingdale, New York) to remove all traces of organic solvent and redissolved in an equal volume of 30% aqueous acetonitrile, 0.1% TFA. Unmodified ParR dimers were analyzed with SA (20 μg/μL) dissolved in 70% aqueous acetonitrile, 0.1% TFA; and DTSSP-cross-linked ParR dimers were analyzed with DHB dissolved in 30% aqueous acetonitrile, 0.1% TFA.

Preparation of MALDI-MS samples

Prior to MALDI-MS analysis, all ParR protein and peptide samples were desalted and concentrated on disposable microcolumns (Gobom et al., 1997) packed with POROS R2 50 (protein) or POROS R2 20 (peptides) reverse-phase media (PerSeptive Biosystems, Cambridge, Massachusetts). Peptide samples from the in situ digests were desalted and concentrated on disposable nanocolumns (volume ~ 100 nL) (Gobom et al., 1998) packed with POROS R2 10 reverse-phase media (PerSeptive Biosystems, Cambridge, Massachusetts). The peptides bound to the reverse-phase media were washed with 10 μL 0.1% TFA, and eluted onto the MALDI-MS target with matrix solution (two to three droplets of ~100 nL).

Preparation of ESI-MS samples

Prior to ESI-MS analysis, the ParR peptide digest was desalted and concentrated on a disposable microcolumn (Gobom et al., 1997) packed with POROS R2 20 reverse-phase media (PerSeptive Biosystems, Cambridge, Massachusetts). The bound peptides were washed with 10–20 μL 1% formic acid and eluted into precoated borosilicate nanoelectrospray needles (MDS Protana A/S, Odense, Denmark) with 1–2 μL 50% aqueous MeOH, 1% formic acid.

MALDI-TOF-MS analyses

Mass spectra were recorded on a Voyager Elite MALDI reflector time-of-flight (MALDI-RE-TOF) mass spectrometer (PerSeptive Biosystems, Cambridge, Massachusetts) equipped with a 337 nm nitrogen laser and a delayed-extraction ion source. Positively charged ions were analyzed in reflector and linear mode. For the MALDI-

TOF-MS analysis of the ParR protein and ParR tryptic digests, half a microliter of desalted sample was mixed with an equal volume of matrix solution and deposited onto the stainless steel MALDI target. Cocrystallization of the matrix and sample occurred at ambient temperature (Kussmann et al., 1997). Spectra were acquired as the sum of ions generated by irradiation of the sample with 64 to 128 laser shots. An acceleration voltage of 20–25 keV in linear mode was applied for analysis of the intact ParR protein. All peptide analyses were performed in reflector mode with an acceleration voltage of 20 kV. External calibration for ParR was accomplished using the average masses of unmodified ParR protein monomer. Internal calibration for digests of the cross-linked ParR dimer and the CD28–CD80 heterodimer were achieved using the known monoisotopic masses of specified tryptic fragments of the proteins.

ESI-Q-TOF-MS-MS analyses

Electrospray ionization tandem mass spectrometry (ESI-MS-MS) was performed using a quadrupole time-of-flight (Q-TOF) mass spectrometer (Micromass, Wythenshawe, United Kingdom) equipped with an atmospheric nanoelectrospray ionization source. Optimal transmission of the ion beam into the mass spectrometer was achieved via a hexapole transfer lens. The source temperature was 40 °C, and a N_2 gas flow rate of 50 L/h was used to desolvate the charged droplets produced in the source. A voltage of 55 V was applied to the cone and remained unaltered during the analysis. Without applied N_2 back pressure, the capillary needle containing the desalted peptide mixture was opened by gently breaking the tip on the metal face of the cone. Once flow was initiated (~10–30 nL/min), a potential of 800 V was applied to the capillary and the back pressure was adjusted to produce a stable spray (~5–6 psi). A quadrupole analyzer was used to select the doubly charged precursor ion for fragmentation in the hexapole collision cell. Resolution in the quadrupole was set to a minimum to allow maximum transmission of the ion beam into the collision cell but preventing transmission of contaminating ions. The collision gas was argon at a pressure of $\sim 6 \times 10^{-5}$ mbar and a collision energy of 30 V was used to fragment the precursor ions. Product ions were analyzed using an orthogonal reflector TOF analyzer, a microchannel plate, and a time-to-digital (TDC) converter. Product-ion spectra were recorded in positive-ion mode from m/z 50–2,000, and the signal was accumulated over 50–100 scans in the continuum acquisition mode. The acquisition of the data was performed on a MassLynx Windows NT PC data system. External calibration was achieved using a multipoint calibration with NaI (1 μg/μL in 50% aqueous isopropanol). The mass accuracy for tandem MS experiments was within 0.05 m/z units.

Data analyses

MALDI mass spectra were processed using the GRAMS/386 software (Galactica Industries Corp., Salem, New Hampshire) and peptide mapping data evaluated with the General Peptide Mass Analysis for Windows (GPMAW) software, Version 3.12 (Lighthouse Data, Odense, Denmark). The introduction of user-defined protein modifications and cross-links aided analysis of complex MALDI-MS digest spectra, i.e., the mass increments for the reduced and hydrolyzed forms of DTSSP and for the intra- and intermolecular cross-links (see Fig. 3) were defined and assigned to lysine residues. The GPMAW program compared experimentally obtained peptide maps with predicted proteolytic digests and assigned molecular ions in the peptide map to unmodified, cross-linked, and surface-labeled peptides of the protein of interest. ESI-MS-MS spectra were analyzed using the BioLynx function of the MassLynx Version 3.2 Build 004 software (Micromass, Wythenshawe, United Kingdom).

Acknowledgments

K.L. Bennett and M. Kussmann contributed equally to this work. The authors would like to thank Rasmus Bugge Jensen and Kenn Gerdes for scientific discussion, Kate Rafn and Søren Andersen for technical assistance, the Danish Research Academy (Forskerakademiet) and Active Biotech Research AB, Lund, Sweden for Postdoctoral Fellowship funding (K.L.B. and M.K., respectively), and the Danish Biotechnology Program for additional financial support. This study is part of the activities of the Centre for Experimental Biotechnology (CEBI) sponsored by the Danish National Research Foundation.

References

Artemyev NO, Mills JS, Thornburg KR, Knapp DR, Schey KL, Hamm HE. 1993. A site on transducin α-subunit of interaction with the polycationic region of cGMP phosphodiesterase inhibitory subunit. *J Biol Chem 268*: 23611–23615.

Ayed A, Krutchinsky AN, Ens W, Standing KG, Duckworth HW. 1998. Quantitative evaluation of protein–protein and ligand–protein equilibria of a large allosteric enzyme by electrospray ionisation time-of-flight mass spectrometry. *Rapid Commun Mass Spectrom 12*:339–344.

Cohen LRH, Strupat K, Hillenkamp F. 1997. Analysis of quaternary protein ensembles by matrix assisted laser desorption/ionisation mass spectrometry. *J Am Soc Mass Spectrom 8*:1046–1052.

Davies GE, Stark GR. 1970. Use of dimethyl suberimidate, a cross-linking reagent, in studying the subunit structure of oligomeric proteins. *Proc Natl Acad Sci USA 66*:651–656.

Farmer TB, Caprioli RM. 1998. Determination of protein–protein interactions by matrix-assisted laser desorption/ionisation mass spectrometry. *J Mass Spectrom 33*:697–704.

Gobom J, Nordhoff E, Ekman R, Roepstorff P. 1997. Rapid micro-scale proteolysis of proteins for MALDI-MS peptide mapping using immobilised trypsin. *Int J Mass Spectrom Ion Processes 169/170*:153–163.

Gobom J, Nordhoff E, Mirgorodskaya E, Ekman R, Roepstorff P. 1998. Sample purification and preparation technique based on nano-scale reversed-phase columns for the sensitive analysis of complex peptide mixtures by matrix-assisted laser desorption/ionisation mass spectrometry. *J Mass Spectrom 34*:105–116.

Greenfield EA, Nguyen KA, Kuchroo VK. 1998. CD28/B7 costimulation: A review. *Crit Rev Immunol 18*:389–418.

Haniu M, Horan T, Arakawa T, Le J, Katta V, Rohde MF. 1995. Extracellular domain of granulocyte-colony stimulating factor receptor: Interaction with its ligand and identification of a domain in close proximity of ligand-binding region. *Arch Biochem Biophys 324*:344–356.

Hegyi G, Mák M, Kim E, Elzinga M, Muhlrad A, Reisler E. 1998. Intra-strand cross-linked actin between Gln-41 and Cys-374. I. Mapping of sites cross-linked in F-actin by *N*-(4-azido-2-nitrophenyl) putrescine. *Biochemistry 37*:17784–17792.

Helin J, Caldentey J, Kalkkinen N, Bamford DH. 1999. Analysis of the multimeric state of proteins by matrix assisted laser desorption/ionisation mass spectrometry after cross-linking with glutaraldehyde. *Rapid Commun Mass Spectrom 13*:185–190.

Jensen RB, Lurz R, Gerdes K. 1998. Mechanism of DNA segregation in prokaryotes: Replication pairing by *parC* of plasmid R1. *Proc Natl Acad Sci USA 95*:8550–8555.

Jung SM, Moroi M. 1983. Cross-linking of platelet glycoprotein Ib by *N*-succinimidyl(4-azidophenyldithio)propionate and 3,3-dithiobis(sulfosuccinimidyl propionate). *Biochim Biophys Acta 761*:152–162.

Kaufmann R, Kirsch D, Tourmann JL, Machold J, Hucho F, Utkin Y, Tsetlin V. 1995. Matrix-assisted laser desorption ionisation (MALDI) and post-source decay (PSD) product ion mass analysis localise a photolabel crosslinked to the delta-subunit of nAChR protein by neurotoxin II. *Eur Mass Spectrom 1*:313–325.

Kussmann M, Nordhoff E, Rahbek-Nielsen H, Haebel S, Rossel-Larsen M, Jakobsen L, Gobom J, Mirgorodskaya E, Kroll-Kristensen A, Palm L, Roepstorff P. 1997. Matrix-assisted laser desorption/ionisation mass spectrom-

etry sample preparation techniques designed for various peptide and protein analytes. *J Mass Spectrom 32*:593–601.
Laemmli UK. 1970. Cleavage of structural proteins during the assembly of the head of bacteriophage T_4. *Nature 277*:680–685.
Leffak IM. 1983. Decreased protein staining after chemical crosslinking. *Anal Biochem 135*:95–101.
Lomant AJ, Fairbanks G. 1976. Chemical probes of extended biological structures: Synthesis and properties of the cleavable protein crosslinking reagent (^{35}S)dithiobis(succinimidyl proprionate). *J Mol Biol 104*:243–261.
Loo JA. 1997. Studying noncovalent protein complexes by electrospray ionisation mass spectrometry. *Mass Spectrom Rev 16*:1–23.
Machold J, Utkin Y, Kirsch D, Kaufmann R, Tsetlin V, Hucho F. 1995. Photolabelling reveals the proximity of the α-neurotoxin binding site to the M2 helix of the ion channel in the nicotinic acetylcholine receptor. *Proc Natl Acad Sci USA 92*:7282–7286.
Metzler WJ, Bajorath J, Fenderson W, Shaw SY, Constantine KL, Naemura J, Leytze G, Peach RJ, Lavoie TB, Mueller L, Linsley PS. 1997. Solution structure of human CTLA-4 and delineation of a CD80/CD86 binding site conserved in CD28. *Nat Struct Biol 4*:527–531.
Mills JS, Miettinen HM, Barnidge D, Vlases MJ, Wimer-Mackin S, Dratz EA, Sunner J, Jesaitis AJ. 1998. Identification of a ligand binding site in the human neutrophil formyl peptide receptor using a site-specific fluorescent photoaffinity label and mass spectrometry. *J Biol Chem 273*:10428–10435.
Neubauer G, King A, Rappsilber J, Calvio C, Watson M, Ajuh P, Sleeman J, Lamond A, Mann M. 1998. Mass spectrometry and EST-database searching allows characterisation of the multi-protein spliceosome complex. *Nat Genet 20*:46–50.
Ngai S-M, Sönnichsen FD, Hodges RS. 1994. Photochemical cross-linking between native rabbit skeletal troponin C and benzoylbenzoyl-troponin I inhibitory peptide, residues 104–115. *J Biol Chem 269*:2165–2172.
Patterson SD, Katta V. 1994. Prompt fragmentation of disulphide-linked peptides during matrix-assisted laser desorption ionisation mass spectrometry. *Anal Chem 66*:3727–3732.
Roepstorff P, Fohlman J. 1984. Proposal for a common nomenclature for sequence ions in mass spectra of peptides. *Biomed Mass Spectrom 11*:601.
Rosinke B, Strupat K, Hillenkamp F, Rosenbusch J, Dencher N, Kruger U, Galla HJ. 1995. Matrix-assisted laser desorption/ionisation mass spectrometry (MALDI-MS) of membrane proteins and non-covalent complexes. *J Mass Spectrom 30*:1462–1468.
Rossi V, Gaboriaud C, Lacroix M, Ulrich J, Fontecilla-Camps JC, Gagnon J, Arlaud GJ. 1995. Structure of the catalytic region of human complement protease C1s: Study by chemical cross-linking and three-dimensional homology modelling. *Biochemistry 34*:7311–7321.
Scaloni A, Miraglia N, Orrù S, Amodeo P, Motta A, Marino G, Pucci P. 1998. Topology of the calmodulin-melittin complex. *J Mol Biol 277*:945–958.
Shevchenko A, Wilm M, Vorm O, Mann M. 1996. Mass spectrometric sequencing of proteins from silver stained polyacrylamide gels. *Anal Chem 68*:850–858.
van der Merwe PA, Bodian DL, Daenke S, Linsley P, Davis SJ. 1997. CD80 (B7-1) binds both CD28 and CTLA-4 with a low affinity and very fast kinetics. *J Exp Med 185*:393–403.
Vater J, Heinze K, Friedrich B, Kablitz B, Blokesch A, Irrgang K-D, Thiede B, Salnikow J. 1996. Novel methodology for topological studies of photosynthetic membrane protein complexes. *Ber Bunsenges Phys Chem 100*:2107–2111.
Yang T, Horejsh DR, Mahan KJ, Zaluzec EJ, Watson TJ, Gage DA. 1996. Mapping cross-linking sites in modified proteins with mass spectrometry: An application to cross-linked haemoglobins. *Anal Biochem 242*:55–63.
Yu ZH, Friso G, Miranda JJ, Patel MJ, Lotseng T, Moore EG, Burlingame AL. 1997. Structural characterisation of human haemoglobin crosslinked by bis(3,5-dibromosalicyl) fumarate using mass spectrometric techniques. *Protein Sci 6*:2568–2577.
Zappacosta F, Ingallinella P, Scaloni A, Pessi A, Bianchi E, Sollazzo M, Tramontano A, Marino G, Pucci P. 1997. Surface topology of minibody by selective chemical modifications and mass spectrometry. *Protein Sci 6*:1901–1909.